Int. J. Solids Structures Vol. 16, pp. 301–312
Pergamon Press Ltd., 1980. Printed in Great Britain

ULTRASONIC WAVE PROPAGATION IN A RANDOM PARTICULATE COMPOSITE

VIKRAM K. KINRA,† MARTIN S. PETRAITIS‡ and SUBHENDU K. DATTA
Department of Mechanical Engineering, University of Colorado, Boulder, CO 80309, U.S.A.

(*Received* 11 *January* 1979; *in revised form* 14 *June* 1979)

Abstract—Ultrasonic wave propagation in a composite consisting of spherical glass inclusions distributed in a random homogeneous manner in an epoxy matrix has been studied in the frequency range of 0.3–5 MHz. The longitudinal and shear phase velocities, and the attenuation of longitudinal waves in the composite were determined as functions of frequency and the volume fraction of the inclusions.

The results are compared with several theoretical analyses available in the literature. It is shown that the results of Datta are in very good agreement with the experimental observations. Further, the data satisfy the bounds due to Hashin and Shtrikman, and due to Miller. The phenomenon of cut-off frequencies—a characteristic of *periodic* composites—is *not* observed in the *random* particulate composities.

1. INTRODUCTION

Considerable advances have been made in the technology of composite materials in recent years. These composites may be broadly classified into three categories: Plate, Fibrous and Particulate composites. The first two have received considerable attention in the past; however, it is only recently that the particulate composites—consisting of particles of one material dispersed in the matrix of a second—have begun to receive attention. Although some theoretical works dealing with random particulate composites have appeared in the literature, no experimental work in this area has been reported.

Among the theoretical analyses of wave propagation in random particulate composites may be mentioned the works of Datta[1, 2] and Mal and Bose[4]. Datta [1, 2] treated the problem of plane longitudinal and shear wave propagation in a composite made of aligned elastic ellipsoids in welded contact with an elastic matrix. Mal and Bose[4], on the other hand, presented the solution for the case of spherical particles in viscous contact with the matrix. Because of the complexity of the problem, several simplifying assumptions were made in[1–4]. They are:

(1) It was assumed that the distribution of the inclusions was homogeneous and uncorrelated.

(2) Lax's "quasi-crystalline approximation" was used. This approximation is based on the assumption that,

$$\langle u_j \rangle_{ij} = \langle u_j \rangle_j,$$

where $\langle u_j \rangle_{ij}$ is the ensemble average of a field quantity at the jth scatterer position keeping the ith and jth scatterers fixed in position.

(3) It was further assumed that an effective plane wave moves through the medium with a characteristic wave speed, namely, "the effective wave speed."

Even with these simplifying assumptions, the problem of ellipsoidal inclusions is algebraically rather complicated. For this reason, a further simplifying assumption was made in[1, 3]: the effective field as seen by the ith scatterer is a plane wave moving at the effective wave speed in the composite. This resulted in relatively simpler expressions for the two effective wave speeds. However, it should be mentioned that this assumption is reasonable only for low concentrations of the inclusions, as will be seen when the results are compared with the experiments. The final results of [1, 2] are reproduced in Appendix 1, together with their limiting forms for the spherical inclusions. It may be noted that the results presented in [4] for viscous contact can be specialized to give those for the welded contact and these agree with the results of [2]. The

†Author for correspondence.
‡Present address: National Semiconductors, Santa Clara, CA 95050, U.S.A.

expressions for *static* effective elastic modulii derived by Chen and Acrivos[8] are also reproduced in Appendix 1.

This paper is concerned with an experimental investigation of wave propagation in random particulate composites with a view to assessing the range of validity of the theoretically produced results. The composite used here consists of spheres of glass dispersed in a random homogeneous manner in an epoxy. The longitudinal and the shear wave phase velocities, $\langle c_1 \rangle$ and $\langle c_2 \rangle$ and the attenuation of the longitudinal waves, $\langle \alpha \rangle$, are measured over the ultrasonic frequency range 0.3–5 MHz. The experimental results are compared with the predictions of[1, 2]. It is shown that the agreement with [2] is quite good; however, the agreement with [1] is not so good at high concentration. This is not at all surprising in view of the discussion above. Finally, the experimental results are also compared with the bounds on effective modulii of Hashin and Shtrikman[5], Walpole[6] and Miller[7], and with the recent calculations of the static effective elastic modulii by Chen and Acrivos[8].

2. EXPERIMENTAL PROCEDURES

A through-transmission water-immersion ultrasonic tank was used in this investigation (see Fig. 1). The apparatus was built around a pair of accurately matched wide-band piezoelectric ultrasonic transducers[9]. Distilled water was used as the immersion liquid for the following reasons: it has good acoustic coupling with both the transducers and the specimen; it serves as the coolant and it is readily available. The Pulse Generator (Tektronix Type PG 501) was triggered by the output of the Time Mark Generator (Tek. TM 184); the duration of the pulse was varied between 10 μsec and 50 μsec. This pulse was then applied to the Function Generator (Tek. FG 502), which produced a tone-burst of the desired center frequency. The tone-burst was amplified by the Power Amplifier (E.I.N. Radio Frequency 310L) to a peak-to-peak voltage ranging from 40 to 80 volts and then applied to the transmitting transducer. The frequency of the tone-burst was kept close to the center frequency of the transducers. The signal received by the receiving transducer was displayed on the Oscilloscope (Tek. 7403 with 7B53A Delay Time Base Unit and 7A13 Differential Comparator) (see Fig. 2).

In this investigation we are concerned only with the *phase* velocity, rather than with the group velocity. Therefore, all measurements were made with a specific peak near the center of the tone-burst, where the signal had reached a steady state. Furthermore, it was ensured that the peak was at least 5–10 cycles away from both the head and the tail of the tone-burst. The phase velocity $\langle c_1 \rangle$ was measured in the following manner.

With the specimen removed, let t_1 and t_2 be respectively the arrival times of the specific peak when the transducers are d_1 and d_2 apart ($t = 0$ is defined to be the time when the Pulse Generator is triggered). Let t_3 be the arrival time with specimen in place and transducers d_2

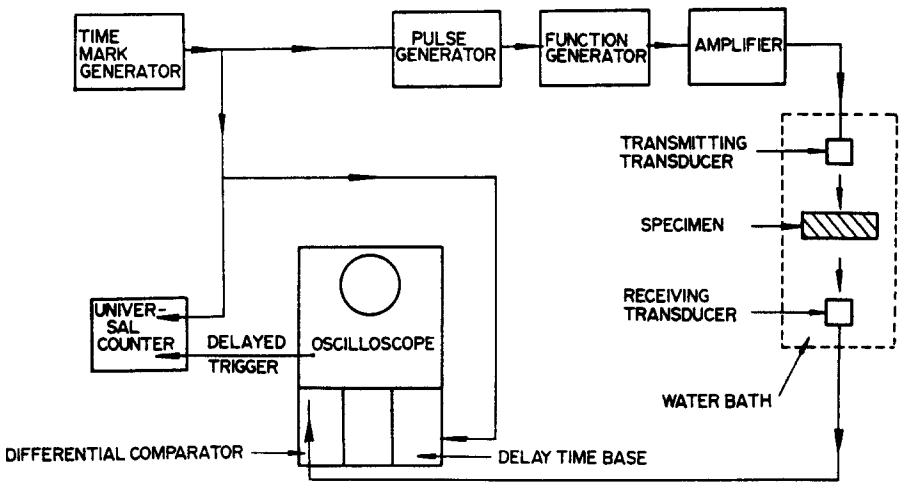

Fig. 1. Schematic of the apparatus.

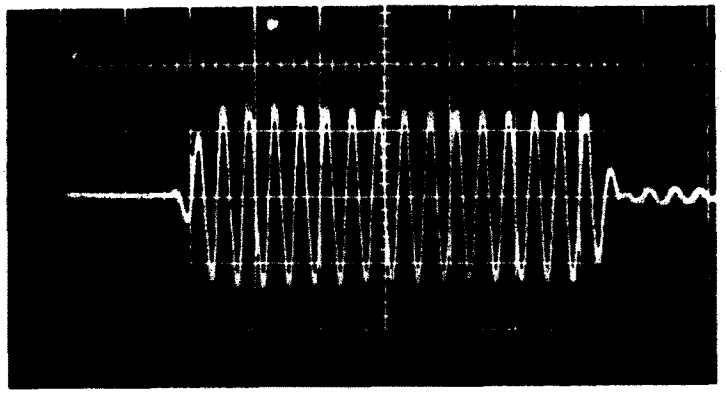

Fig. 2. A typical tone-burst signal received through the composite ($\bar{c} = 0.086$, $n = 0.5$ MHz, horizontal = 5 μsec, vertical = 0.2 volts).

apart; let w be the specimen thickness and $\Delta d = d_2 - d_1 > 0$, then,

$$\langle c_1 \rangle^{-1} = \langle S_1 \rangle = (t_2 - t_1)/\Delta d + (t_3 - t_2)/w. \tag{1}$$

It is well known that the sound velocity in water varies appreciably with temperature. This source of error was eliminated by measuring the velocity in water in each experiment (the first term in eqn (1) is the slowness in water). Shear waves in the composite were generated by mode conversion: the specimen was rotated about a vertical axis until the received signal corresponding to the shear wave exhibited an approximate maximum (the signal corresponding to the longitudinal wave in the specimen at this incident angle was negligibly small). The angle of incidence, i, was measured to the nearest degree and the angle of refraction, r, for the shear waves was calculated by,

$$\tan(r) = w \sin(i)/(w \cos(i) - \Delta t V_w), \tag{2}$$

where $V_w = (d_2 - d_1)/(t_2 - t_1)$ is the velocity of sound in water and $\Delta t = t_2 - t_3$. Finally,

$$\langle c_2 \rangle = V_w \sin(r)/\sin(i). \tag{3}$$

In the foregoing, we have assumed that when a plane pressure wave is obliquely incident upon a particulate composite, the transmitted P- and S-waves are also plane.

The arrival times t_1, t_2 and t_3 were measured as follows. The signal applied to the transmitter was displayed on the upper beam. The received signal was displayed on the lower beam. However, in order to display this signal at an appropriately fast sweep, the triggering of the lower beam was suitably delayed. The delay-time was adjusted until the specific peak occupied (say) the center graticule of oscilloscope grid as viewed with an 8× magnifying glass. The delay-time was accurately measured with the Counter/Timer (Tek. DC505) to an accuracy of ± 1 nanosec. A major advantage of this technique is that it permits online measurements of the wave velocities; human errors could, therefore, be completely eliminated. A systematic error analysis has been carried out in Appendix 2; it is shown that the velocity measurements are accurate to within ± 1%.

The attenuation measurements were made with two specimens of different thicknesses, w_1 and w_2. Let the corresponding amplitudes of the specific peak be A_1 and A_2. Then, the attenuation

$$\langle \alpha \rangle = \ln(A_1/A_2)/(w_2 - w_1) \text{ nepers/mm}. \tag{4}$$

The inaccuracies in $\langle \alpha \rangle$ range from 6% to 15% (see Appendix 2).

Specimen preparation. The specimens consisted of spheres of glass of mean radius a =

150 μm dispersed in an epoxy matrix (TRA-CAST 3012). Ideally, an elastic material should be used for the matrix. However, this presented insurmountable manufacturing difficulties and the epoxy was used instead.

Although the epoxy must be viewed as a linear viscoelastic material, it was found that over the range of frequencies used, $0.3 \leq n \leq 5$ MHz, both c_1 and c_2 are independent of n. Further, $\alpha \ll \langle\alpha\rangle$, implying that in the composite, the scattering effects dominate the viscoelastic effects. It is assumed, therefore, that it is valid to compare the results of these experiments with the analysis of elastic–elastic composites.

A brief description of the epoxy and its curing process is given in [10]. The choice of radius of the glass spheres[11] was governed by the following considerations.

The analyses[1–4] assume $\lambda \gg a$, where λ is any of the four wavelengths λ_1, λ_2, λ_1' and λ_2', where $(\,)'$ denotes the inclusion and the subscripts $(\,)_1$ and $(\,)_2$ denote, respectively, the longitudinal and the shear disturbances. For $0.3 \leq n \leq 5$ MHz, we find $1.02 \leq \lambda_1' \leq 16.93$ mm, $0.67 \leq \lambda_2' \leq 11.16$ mm, $0.51 \leq \lambda_1 \leq 8.47$ mm and $0.232 \leq \lambda_2 \leq 3.87$ mm; thus the conditions $\lambda \gg a$ are satisfied.

Early attempts to prepare the specimen in a single casting operation failed because of settling of glass particles during the curing process. This difficulty was overcome by preparing the specimen in several steps as described below. The desired cross section dimensions of the specimens were 50×50 mm. We started by pouring epoxy in a mold 178×178 mm; the thickness of the epoxy was kept nearly equal to the mean inter-particle distance d, given in terms of the volume fraction of the inclusions, $\bar{c}$, by:

$$d = a(4\pi/3\bar{c})^{1/3}. \tag{5}$$

Here, d was calculated on the assumption that the inclusions are arranged in a simple cubic structure. $\bar{c}$ varied from 0.086 to 0.533 and accordingly d varied from 300 to 560 μm. When the epoxy was roughly half-cured and hence had attained rather large viscosity, the measured amount of glass balls was dispersed into the layer. The balls sank to the bottom but were constrained from lateral movement by the high viscosity. This prevented clustering of the balls, although some of it always occurred even at low volume fractions. Since a single layer was found to be too thin for the subsequent machining operations, four layers were consecutively cured on top of each other; the curing of the second layer was started only after the first one had fully cured and so on. This four-lamina sheet was cut into 9 squares (50×50 mm). These squares were randomly stacked, a thin film of matrix epoxy was applied to the mating surfaces, the assemblage was subjected to an appropriate pressure and the curing cycle repeated. Finally, the faces of the specimens were polished and lapped parallel to 25 μm. The exact volume fraction, $\bar{c}$, of the machined specimen was determined by measuring independently the densities of the specimen, the matrix and the glass spheres.

A visual examination of the composite revealed that the particles were, in fact, distributed in a fairly random manner, although some clustering occurred even at low volume fractions. In order to estimate the influence of this and several other minor sources of errors, the following routine test was undertaken. Two of us independently prepared the specimens with same concentration and made independent measurements of wave velocities. The results agreed within the estimates of error (1%; see Appendix 2).

3. RESULTS AND DISCUSSIONS

3.1 *Properties of the constituents*

Several specimens with thickness ranging from about 15 mm to 50 mm were cast from the epoxy alone. The wave velocities and the attenuation were measured over the frequency range $n = 0.3$ to 5 MHz. It was found that both c_1 and c_2 are independent of frequency: $c_1 = 2.54$ mm/μsec and $c_2 = 1.16$ mm/μsec. Since thicker specimens were used, these measurements are accurate to $\pm 0.3\%$, compared to $\pm 1\%$ for the composites. The attenuation α increased linearly with n. The results of a linear regression are: $\alpha = mn + \alpha_0$, where n is in MHz; $m = 0.0456$ nepers/(mm–MHz), and the intercept $\alpha_0 = 0.001$ nepers/mm. The reduced data is plotted in Figs. 9 and 10. Furthermore, several measurements were carried out with samples of

Aluminum 6061-T6 and EPON 828-Z epoxy. The results are compared in Table 1 with those available in the literature, confirming our estimates of accuracy. Finally, the properties of the constituents are given in Table 2.

3.2 *Velocity measurements*

Five specimens were prepared with $\bar{c} = 0.086, 0.164, 0.351, 0.451$ and 0.533. For the lowest $\bar{c}$, $d/a = 3.73$, hence it may be considered a dilute suspension of inclusions. Some specimens with even lower $\bar{c}$ were prepared; however, it was found that very much thicker specimens are needed to make accurate measurements because of very small differences between $\langle c_1 \rangle$ and c_1 at these volume fractions. At the other end, $\bar{c} = 0.533$, $d/a = 1.98$. (We note for comparison that for a close-packed simple cubic structure $d/a = 2.0$ and $\bar{c} = 0.524$.)

Four pairs of transducers were used in this investigation. For each pair, a center frequency was determined experimentally, based on the criterion that the transients at the head and tail of the tone-burst attenuate most rapidly. The center frequencies were found to be 0.4, 0.8, 2.3 and 3.5 MHz. The dimensionless longitudinal velocity $\langle c_1 \rangle / c_1$, measured at these frequencies, is plotted in Figs. 3–6 as a function of $\bar{c}$.

If Fig. 3, the experimental results at 0.4 MHz are compared with the analysis of Datta[2]. Let $\delta = \lambda/a$, then $\delta_1' = 85$, $\delta_2' = 56$, $\delta_1 = 42$, $\delta_2 = 19$; thus the long wavelength assumption of the analysis is adequately satisfied. The comparison is considered excellent up to $\bar{c} = 0.451$. At $\bar{c} = 0.533$, there is a steep rise in the experimental $\langle c_1 \rangle / c_1$ and the discrepancy becomes significant. This is not at all surprising, since at this volume fraction a large fraction of particles were observed to be in direct contact—a fact not taken into account in the analysis. It is reassuring to note that the experimental $\langle c_1 \rangle$ is *larger* than the predicted one, because heuristically one would expect the direct contact to lend greater stiffness to the composite. This observation may be seen to hold for all frequencies tested (Figs. 3–7). In Fig. 4, a similar

Table 1. Comparison of values obtained in this study with values obtained in other studies

	This work				Other work			
Specimen	Specific gravity	c_1 mm/μsec	c_2 mm/μsec	α Nepers mm	Specific gravity	c_1 mm/μsec	c_2 mm/μsec	α Nepers mm
AL 6061-T6	2.700	6.38	3.09		2.693†	6.40†	3.1§	—
EPON-828-Z	1.202	2.64	—	0.086¶	1.202‡	2.67‡	—	0.082‡,¶

†Ref. [12].
‡Ref. [13].
§Ref. [11].
¶Measurement taken at $n = 2.0$ MHz.

Table 2. Constituent properties

Material-	Young's modulus (psi)	(GPa)	Specific gravity	Poisson's ratio
TRA-CAST	6.25×10^5	4.06	1.18	0.370
Glass	10×10^6	64.89	2.47	0.249

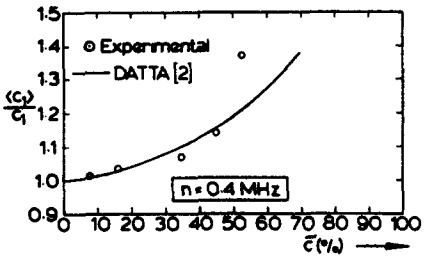

Fig. 3. Longitudinal phase velocity vs volume fraction ($\delta_1 = 42$, $\delta_2 = 19$, $\delta_1' = 85$, $\delta_2' = 56$).

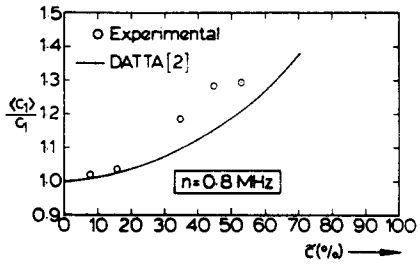

Fig. 4. Longitudinal phase velocity vs volume fraction ($\delta_1 = 21$, $\delta_2 = 10$, $\delta_1' = 42$, $\delta_2' = 28$).

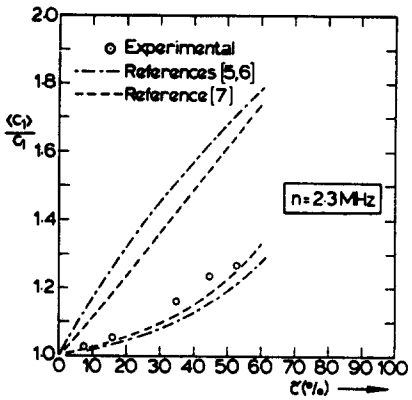

Fig. 5(a). Logitudinal phase velocity vs volume fraction ($\delta_1 = 7$, $\delta_2 = 3.4$, $\delta_1' = 15$, $\delta_2' = 10$).

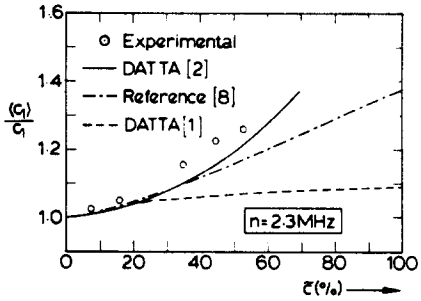

Fig. 5(b). Longitudinal phase velocity vs volume fraction ($\delta_1 = 7$, $\delta_2 = 3.4$, $\delta_1' = 15$, $\delta_2' = 10$).

comparison is shown for $n = 0.8$ MHz. At low volume fractions the comparison is excellent; however, the discrepancy increases with $\bar{c}$.

In Fig. 5(a), the measurements at 2.3 MHz are compared with the bounds of Hashin and Shtrikman[5] for a general two-phase material and with the bounds of Miller[7] for *spherical* inclusions. Since Miller's calculations are restricted to effective bulk modulus only, in order to calculate $\langle c_1 \rangle$ the shear modulus bounds were taken from [5]. It is noted the bounds of [5] and [6] are identical. The effective wave speeds corresponding to these bounds were calculated by $\langle c_1 \rangle^2 = (\langle k \rangle + 4/3\langle \mu \rangle)/\langle \rho \rangle$ and $\langle c_2 \rangle^2 = \langle \mu \rangle/\langle \rho \rangle$, where $\langle \rho \rangle = (1 - \bar{c})\rho + \bar{c}\rho'$. The experimental data satisfy both sets of bounds[5–7]; it is, however, interesting to note that the data are very much closer to the lower rather than to the upper bounds. This is to be expected, for as noted by Hashin[17]:

"...intuitively, for two materials with same volume fractions and same phase modulii, where in the first the stiffer phase is a matrix while in the second the more compliant phase is a matrix, the actual effective modulii of the first material will be closer to the upper bound while those of the second will be closer to the lower bound."

For our case, the compliant phase constitutes the matrix.

The data of Fig. 5(a), at 2.3 MHz, is compared in Fig. 5(b) with the calculations of Datta[1, 2] and Chen and Acrivos[8]. At low volume fractions all three analyses predict the experiments rather well. The analysis[1] due to Datta is claimed to be accurate only at low concentrations; this is borne out be the experiments. The *static* results of Chen and Acrivos for spherical inclusions—accurate to $(\bar{c})^2$—compares favorably up to moderate volume fractions as expected. The comparison with Datta[2], which is accurate at least to $(\bar{c})^2$, is the most favorable for the entire range of volume fractions: the maximum discrepancy is about 3% at $\bar{c} = 0.451$.

Figure 6 is a comparison of data at 3.5 MHz with Datta[2]. Here $\delta_1' = 10$, $\delta_2' = 6$, $\delta_1 = 5$ and $\delta_2 = 2.2$, i.e. the shortest of the wavelengths, namely shear wavelength, in the matrix is almost equal to the particle diameter. It is, therefore, very surprising to note that the analysis[2] predicts very well the observed results. Clearly, the results of[2] are valid at least somewhat outside the range of the underlying assumption of long wavelengths. Unfortunately, due to anticipated poor signal-to-noise ratio resulting from increased attenuation, measurements were

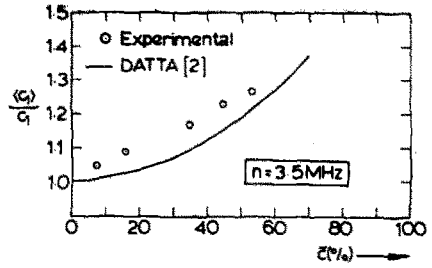

Fig. 6. Longitudinal phase velocity vs volume fraction ($\delta_1 = 5$, $\delta_2 = 2.2$, $\delta_1' = 10$, $\delta_2' = 6$).

not attempted at higher frequencies, i.e. lower wavelengths. It would be extremely interesting to probe the regime δ_1, δ_2, δ_3, $\delta_4 \sim 1$ with a view to comparing the results with [2].

The measurements of shear velocity $\langle c_2 \rangle / c_2$ at 1 MHz are plotted in Fig. 7. Since the excitation of shear waves in the composite involved two mode conversions, the amplitudes of the received signals were very much lower than those for $\langle c_1 \rangle$, hence measurements at $n > 1$ MHz could not be made. The predictions of Datta[1, 2], the bounds due to Hashin and Shtrikman[5] (same as the bounds of Walpole[6]) and calculations of Chen and Acrivos[8] are also included in Fig. 7. Here, as for $\langle c_1 \rangle$, the analysis [1] is in good agreement at dilute concentrations, but deviates significantly as $\bar{c}$ increases. The data satisfies the bounds of [5, 6]; it is closer to the lower bound although not nearly as close as was the case for $\langle c_1 \rangle$. It is also noted that the lower bounds of [5, 6] coincide with the results of Datta [2]. The calculations of Chen and Acrivos are in good agreement only up to moderate concentrations; as $\bar{c}$ increases, the discrepancy becomes large. Finally, the results of Datta[2] compare most favorably with the experimental data for the entire range of $\bar{c}$; the discrepancy, however, is somewhat larger than that observed with $\langle c_1 \rangle$ data.

3.3 *Cut-off frequency*

It is well known that *periodic* composites exhibit the phenomenon of cut-off frequencies (see, e.g. Refs. [14, 15]). For longitudinal waves, the first cut-off frequency corresponds to the condition $\lambda_1 = 2d$, where d is the dimension of the unit cell in the direction of wave propagation. *If the cut-off frequencies exist* in random particulate composites, the first of these, n_c, may be expected to satisfy the condition $\lambda_1 = 2d$, where d is the *mean* interparticulate distance; for each volume fraction tested in this investigation, the n_c, calculated accordingly, is indicated in Fig. 8, where data from Figs. 3–6 has been plotted with n as the independent

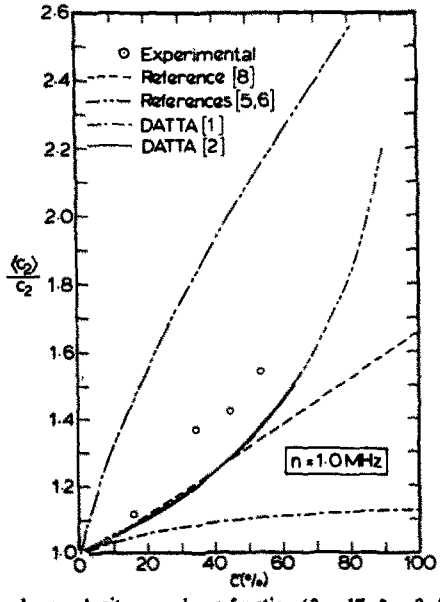

Fig. 7. Shear phase velocity vs volume fraction ($\delta_1 = 17$, $\delta_2 = 8$, $\delta_1' = 34$, $\delta_2' = 22$).

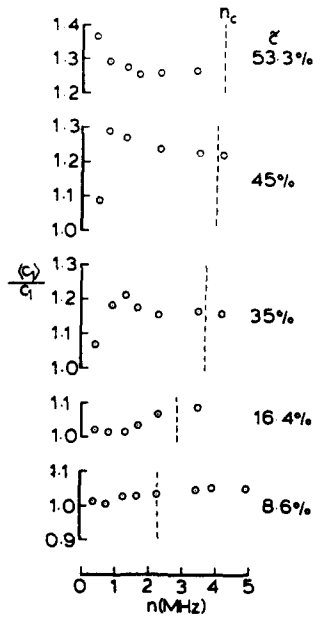

Fig. 8. Longitudinal phase velocity vs frequency.

variable. Following [14, 15], e.g. one would expect a *decrease* in phase velocity as n approaches n_c from below and an *increase* from the other direction. It is evident from Fig. 8 that no sharp changes in $\langle c_1 \rangle$ occur in the vicinity of the calculated n_c. In fact, the only observable trend in the data—and that, too, not very well defined—is the leftward shift of the peak as $\bar{c}$ increases, whereas the calculated n_c shifts to the right. We are led to conclude, therefore, that the random particulate composites do not exhibit the phenomenon of cut-off frequencies. (It will be shown in the sequel that this conclusion is also supported by the attenuation measurements.)

3.4 *Attenuation measurements*

The attenuation $\langle \alpha \rangle$ for $\bar{c} = 0.086$ is shown in Fig. 9; the thicknesses of the specimens were 9.96 and 16.81 mm. The attenuation α for the matrix alone is also shown. Attempts were made to measure the attenuation in glass; it was found to be negligibly small. Since $\langle \alpha \rangle$ is *not* very much larger than α, in order to determine the attenuation due to scattering alone (α_s) the matrix attenuation should be subtracted from $\langle \alpha \rangle$: one plausible *ad hoc* assumption would be to partition $\langle \alpha \rangle$ in proportion to the volume fraction, i.e. $\alpha_s = \langle \alpha \rangle - (1 - \bar{c})\alpha$.

For $\bar{c} = 0.451$, $\langle \alpha \rangle$ is plotted in Fig. 10; the specimen thicknesses were 4.95 and 9.55 mm. At the higher frequencies, $\langle \alpha \rangle \gg (1 - \bar{c})\alpha$ and hence, $\alpha_s \simeq \langle \alpha \rangle$. It is surprising to note that α_s approaches zero at about $n = 1$ MHz rather than at $n = 0$ as expected. However, in order to probe *accurately* the frequency range 0–1 MHz, very much thicker specimens are needed (see

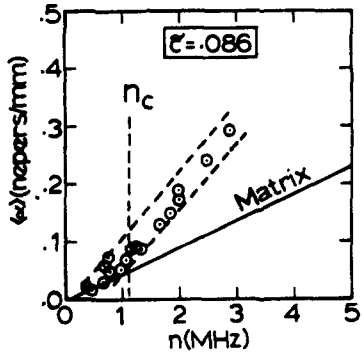

Fig. 9. Attenuation in the composite vs frequency.

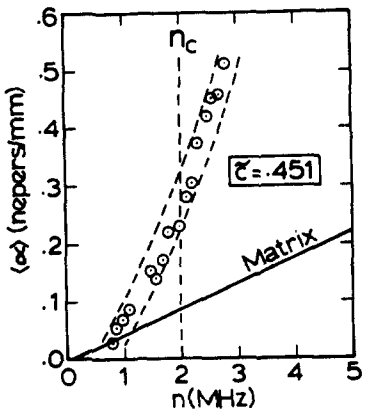

Fig. 10. Attenuation in the composite vs frequency.

Appendix 2) and these are enormously difficult to manufacture (see Section 2). The pairs of broken lines in Fig. 9 and 10 are the error bands; the error ranges from 6 to 15% depending upon frequency and the two thicknesses.

The attentuation data was also collected for the three remaining samples, $\bar{c} = 0.164$, 0.351 and 0.533, but has not been reported for the following reasons. $\bar{c} = 0.533$: the attenuation was very large, therefore, for the thicker specimen signal-to-noise ratio was considered inacceptable. $\bar{c} = 0.164$ and 0.351: here, the reasons are alogether different. In every experiment, in addition to the desired through-transmitted-pulse (TTP), a series of spurious twice-internally-reflected-pulses (TIRP) are also detected. The first of these arrives at $\Delta t = 2w/c_1$ later than TTP. The number of cycles corresponding to Δt is $m = 2wn/c_1$. If TTP had not reached a steady state (Fig. 2) within m cycles from the head of the pulse, the data was considered invalid.

The calculated cut-off frequencies, n_c, are also shown in Figs. 8 and 9. If cut-off frequency exists, then one would expect the attenuation to increase very sharply as n approaches n_c from either side. Clearly, no discernible changes in $\langle\alpha\rangle$ are found, either in the vicinity of n_c or anywhere else in the range of n tested. (In order to preserve clarity, not all the data points are plotted; however, the frequency regime on either side of n_c was very carefully scanned with extremely small increments in frequency and measurements similar to the ones reported were observed.) Therefore, these measurements support our earlier conclusion that *random* particulate composites do not exhibit the phenomenon of cut-off frequencies—at least in the range of frequencies and concentrations tested.

4. CONCLUSIONS

The phase velocities of longitudinal and shear waves, $\langle c_1\rangle$ and $\langle c_2\rangle$ and attenuation of longitudinal waves, $\langle\alpha\rangle$, in a random particulate composite were measured in the frequency (n) range of 0.3–5 MHz and the concentration ($\bar{c}$) range of 8.6–53.3%. The experimental results were found to be in good agreement with the predictions of Datta[1] at low concentrations, with those of Chen and Acrivos[8] up to moderate concentrations and with the results of Datta[2] up to high concentrations. Although the analysis[2] is based on the long-wavelength assumptions, its predictions are in good agreement with the data even when one of the wavelengths becomes comparable to the inclusion dimension. The measured velocities $\langle c_1\rangle$ and $\langle c_2\rangle$ were always larger than those predicted by [1, 2, 8]. The experimental results satisfy the bounds due to Hashin and Shtrikman[5] and Walpole[6] for a *general* two-phase material and the somewhat closer bounds due to Miller[7] for *spherical* inclusions; the data are very much closer to the lower bounds. The phenomenon of cut-off frequencies—a characteristic of *peridoic* composites—was not observed in either the velocity or the attenuation curves for the *random* particular composites. In fact, there is no definitive pattern to the frequency dependence of the velocity. Finally, $\langle\alpha\rangle$ has been reported for $\bar{c} = 0.086$ and 0.451 and $0.3 \leq n \leq 5$ MHz.

Acknowledgements—Thanks are due to Karl Rupp, Charles Coet and Edward McKenna for their technical assistance and to Nickie Ashley for typing the manuscript.

The financial support of the National Science Foundation under the grants ENG-76-09613 and ENG-76-04328 to the University of Colorado is gratefully acknowledged.

REFERENCES

1. S. K. Datta, A. self-consistent approach to multiple scattering by elastic ellipsoidal inclusions. *J. Appl. Mech.* **44**, Trans. *ASME, Series E*, 657–662 (1977).
2. S. K. Datta, Scattering by a random distribution of inclusions and effective elastic properties. *Continuum Model of Discrete Systems* (Edited by J. W. Provan). University of Waterloo Press, 111–127 (1978).
3. S. K. Datta, Scattering of elastic waves by a distribution of inclusions. *Archives Mech.* **28**, 317–324 (1976).
4. S. K. Bose and A. K. Mal, Dynamic elastic moduli of a suspension of imperfectly bonded spheres. *Proc. Cambridge Philosophical Soc.* **76**, 587–600 (1974).
5. Z. Hashin and S. Shtrikman, A variational approach to the theory of the elastic behavior of multiphase materials. *J. Mech. Phys. Solids* **11**, 127 (1963).
6. L. J. Walpole, On bounds for the overall elastic modulii of inhomogeneous systems. *I. J. Mech. Phys. Solids* **14**, 151 (1966).
7. M. N. Miller, Bounds for effective bulk modulus of heterogeneous materials. *J. Math. Phys.* **10**, 2005 (1969).
8. H. S. Chen and A. Acrivos, The effective elastic modulii of composite materials containing spherical inclusions at non-dilute concentrations. *Int. J. Solids Structures* **14**, 349–364 (1978).
9. Panametrics, Inc., 221 Crescent Street, Waltham, Mass. 02154, (617) 899–2719; and Automation Industries, Inc., Sperry Division, Shelter Rock Road, Danbury, CT 06510, (203) 748–3581.

10. TRA-CAST 3012. Manufactured by TRA-CON, Inc., Resin Systems Division, 55 North Street, Medford, Mass. 02155, (617) 391-5540. It is a low viscosity 100% solids (no solvents) epoxy resin and hardener system. Mixing proportions: 46 parts hardener, 100 parts resin. After mixing, the solution was placed in a vacuum chamber until all air was evacuated. The epoxy was then cured for 24 hr at 65°C.
11. Glass particles manufactured by Potters Industries, Inc., 377 Route 17, Hasbrough Heights, N.J. 07604, (201) 288-4700. Product number P-0140. Range of diameter: 250-355 μm, mean diameter: 300 μm.
12. M. P. Felix, Attenuation and dispersion characteristics of various plastics in the frequency range of 1-10 MHz. *J. Comp. Mat.* **8**, 275-287 (1974).
13. H. J. Sutherland and R. Lingle, An acoustic characterization of polymethylmethacrylate and three epoxy formulations. *J. Appl. Phys.* **43**, 4022-4026 (1972).
14. H. J. Sutherland, Geometric dispersion of acoustic waves by a fibrous composite. *J. Comp. Mat.* **6**, 490-502 (1972).
15. E. H. Lee, Wave propagation in composites with periodic structures. *Proc. 5th Canadian Cong. Appl. Mech.* Fredericton, N. B., G49-G59 (1975).
16. J. D. Eshelby, The determination of the elastic field of an ellipsoidal inclusion and related problems. *Proc. R. Soc. London* (A), **241**, 376 (1957).
17. Zvi Hashin, Theory of composite materials. Mechanics of Composite Materials, *Proc. 5th Symposium on Naval Structural Mech.* Philadelphia, 201-242 (1967).

APPENDIX

In this Appendix, we reproduce the final results of Refs. [1, 2, 8]. Consider a random distribution of similar ellipsoidal inclusions with the same orientation embedded in a homogeneous matrix. Let the principal axes of the ellipsoids by $2a$, $2b$, $2c$ with $a \geq b \geq c$. Then it was shown in Ref. [1] that for a longitudinal wave propagating parallel to the c-axis, the effective wave speed $\langle c_1 \rangle$ is given by,

$$\left(\frac{\langle c_1 \rangle}{c_1}\right)^2 = \frac{1 + \bar{c}\left[1 - \bar{T}_{3333} - \frac{\nu}{1-\nu}(\bar{T}_{1133} + \bar{T}_{2233})\right]}{1 + \bar{c}(\rho'/\rho)} \tag{A1}$$

where ρ is the matrix density, $(\ )'$ denotes the inclusion properties, ν is the Poisson's ratio of the matrix and $\bar{T}_{ijkl}$ may be found in [1]. This expression is believed to be accurate for small volume fractions ($\bar{c} \ll 1$). A more accurate relation that is valid at higher concentrations is derived in Ref. [2] and is given by,

$$\begin{aligned}\left(\frac{\langle c_1 \rangle}{c_1}\right)^2 = [1 - \bar{c}\{5T_{02}^{02}(1 + \bar{c}T_{00}^{00}) - T_{02}^{02}(1 + 3\beta^2/2\alpha^2) \\ - (5T_{00}^{02} + T_{02}^{00} + 5\bar{c}T_{00}^{02}T_{02}^{00})\}]/[(1 + 3\bar{c}T_{01}^{00}) \\ \times \{(1 + \bar{c}T_{00}^{00})(1 + \bar{c}T_{02}^{02}(1 + 3\beta^2/2\alpha^2)) - \bar{c}^2 T_{00}^{02}T_{02}^{00} \\ \times (1 + 3\beta^2/2\alpha^2)\}].\end{aligned} \tag{A2}$$

Similar results can be derived for wave propagation along the a- and b-axes. Here $\beta^2/\alpha^2 = 2(1-\nu)/(1-2\nu)$,

$$T_{00}^{00} = \frac{1+\nu}{9(1-\nu)}\bar{T}_{mmnn}, \quad T_{01}^{00} = \frac{1}{3}(\rho'/\rho - 1),$$

$$T_{00}^{02} = \frac{1+\nu}{45(1-\nu)}[\bar{T}_{mmnn} - 3\bar{T}_{mm33}],$$

$$T_{02}^{00} = -\frac{1-2\nu}{3(1-\nu)}\left[\bar{T}_{33nn} - \frac{1}{3}\bar{T}_{mmnn}\right],$$

$$T_{02}^{02} = -\frac{1-2\nu}{15(1-\nu)}\left[\bar{T}_{33nn} - 3\bar{T}_{3333} - \frac{1}{3}(\bar{T}_{mmnn} - 3\bar{T}_{mm33})\right].$$

The constants $\bar{T}_{ijkl}$ are defined by the relation,

$$e_{ij}^T = \bar{T}_{ijkl}e_{kl}^A, \tag{A3}$$

where e_{ij}^A is the applied uniform strain in the matrix at infinity and e_{ij}^T is the transformation strain within the equivalent ellipsoid (see Eshelby [16]).

The corresponding results for propagation of shear waves polarized in the a-direction and propagating in the c-direction are, from Ref. [1],

$$\left(\frac{c_{13}^*}{c_2}\right)^2 = \{1 + \bar{c}(1 - 2\bar{T}_{1313})\}/(1 + \bar{c}\rho'/\rho), \tag{A4}$$

and from Ref. [2],

$$\left(\frac{c_{13}^*}{c_2}\right)^2 = \frac{1 - \bar{c}\frac{4(1-2\nu)}{15(1-\nu)}\bar{T}_{1313}\left(\frac{9\beta^2}{4\alpha^2} - 1\right)}{(1 + 3\bar{c}T_{01}^{00})\left[1 + \bar{c}\frac{4(1-2\nu)}{15(1-\nu)}\bar{T}_{1313}(1 + 3\beta^2/2\alpha^2)\right]}, \tag{A5}$$

where $T^{01}_{01} = T^{11}_{11}$. Note that $c^{\dagger}_3 = c^{\ddagger}_1$, thus there are three shear and three longitudinal wave speeds. For the purpose of this work, we label $c^{\dagger}_3 = \langle c_2 \rangle$.

The above results simplify considerably for the case of spherical inclusions. In this case,

$$\bar{T}_{3333} = (\bar{A} + 2\bar{B})/3, \quad \bar{T}_{1133} = \bar{T}_{2233} = (\bar{A} - \bar{B})/3,$$

$$T^{00}_{00} = (1+\nu)\bar{A}/3(1-\nu), \quad T^{02}_{02} = 2(1-2\nu)\bar{B}/15(1-\nu),$$

$$T^{02}_{00} = T^{00}_{02} = 0, \quad \bar{T}_{1313} = \frac{1}{2}\bar{B}, \quad \bar{A} = \frac{k'/k - 1}{\bar{\alpha}(1 - k'/k) - 1},$$

$$\bar{B} = \frac{\mu'/\mu - 1}{\bar{\beta}(1 - \mu'/\mu) - 1}, \quad \bar{\alpha} = (1+\nu)/3(1-\nu),$$

$\bar{\beta} = 2(4-5\nu)/15(1-\nu)$. Here, k and μ are bulk and shear modulus, respectively.

For very small concentrations $\bar{c}$ both (A1) and (A2) reduce to,

$$\left(\frac{\langle c_1 \rangle}{c_1}\right)^2 = 1 - \bar{c}\left[\frac{\rho'}{\rho} - 1 + \bar{T}_{3333} + \frac{\nu}{1-\nu}(\bar{T}_{1133} + \bar{T}_{2233})\right]. \tag{A6}$$

which is correct to $0(\bar{c})$. Similarly, eqns (A4) and (A5) reduce to,

$$\left(\frac{\langle c_2 \rangle}{c_2}\right)^2 = 1 - \bar{c}[\rho'/\rho - 1 + 2\bar{T}_{1313}]. \tag{A7}$$

Thus the slopes of the curves $\langle c_1 \rangle/c_1$ vs $\bar{c}$ and $\langle c_2 \rangle/c_2$ vs $\bar{c}$ at $\bar{c} = 0$ are, for the spherical inclusions,

$$(1/2)\left[1 - \rho'/\rho - \frac{(1+\nu)\bar{A} + 2(1-2\nu)\bar{B}}{3(1-\nu)}\right] \text{and} \; (1/2)\left[1 - \rho'/\rho - \bar{B}\right],$$

respectively. For the particular materials used in these experiments, these slopes are 0.14 and 0.41 respectively.

The final results of Chen and Acrivos[8] are given next. Let $\langle k \rangle$ and $\langle \mu \rangle$ be, respectively, the static effective bulk and shear modulii, then correct to $(\bar{c})^2$,

$$\frac{\langle k \rangle}{k} = 1 + \left(1 + \frac{4\mu}{3k}\right)\gamma_1 \bar{c} + \left(1 + \frac{4\mu}{3k}\right)(\gamma_1 \bar{c})^2 H_1 + 0(\bar{c}^3), \tag{A8}$$

$$\frac{\langle \mu \rangle}{\mu} = 1 + 15(1-\nu)\gamma_2 \bar{c} + 30(1-\nu)(4-5\nu)(\gamma_2 \bar{c})^2 H_2 + 0(\bar{c}^3), \tag{A9}$$

where

$$\gamma_1 = (3k' - 3k)/(3k' + 4\mu),$$

$$\gamma_2 = (\beta - 1)/[2\beta(4-5\nu) + (7-5\nu)], \text{and} \; \beta = \mu'/\mu.$$

In Ref. ([8], Fig. 1), the numerical results for H_1, as a function of ν, are given for $\nu' = 0.25$ (glass) and several values of β from $\beta = 0$ (cavity) to $\beta = \infty$ ((rigid inclusion). For our case $\beta = 17.55$ and H_1 was determined by interpolation: $H_1 = 1.17$. The results for H_2, on the other hand, were given only for $\beta = 0$ and ∞. Based on the β-dependence of H_1 for the particular $\nu = 0.37$, it is believed that the value of H_2 for $\beta = 17.55$ is not significantly different from that for $\beta = \infty$; thus $H_2 = 1.625$.

APPENDIX 2. ERROR ANALYSIS

1. *Velocity measurements*

We recall eqn (1) for the longitudinal wave speed,

$$\langle c_1 \rangle = \{(t_2 - t_1)/(d_2 - d_1) - (t_2 - t_3)/w\}^{-1}. \tag{B1}$$

Let δt be the random error in measuring t_1, t_2 or t_3. The "reference" peak could be aligned with a vertical line on the graticule with an estimated accuracy of $\pm$ 1/20 division; an 8× magnifying lens was used. The sweep rate was 200 nanosec/division or *faster*. Therefore, the maximum $\delta t = 10$ nanosec. (The error of $\pm$ 1 nanosec caused by the DC505 COUNTER/TIMER has been neglected.) The linear dimensions d_1, d_2 and w were measured to an accuracy better than $\pm$ 0.0254 mm ($\pm 10^{-3}$ in.), hence $\delta(d_1) = \delta(d_2) = \delta(w) = $ (say) $\delta l = \pm 0.0254$ mm. Finally, we make the *conservative* assumption that the *random* error in $\langle c_1 \rangle$ is the absolute—rather than root mean square (RMS)—sum of the component errors, then,

$$\frac{\delta\langle c_1 \rangle}{\langle c_1 \rangle} = \langle c_1 \rangle\left[\frac{2\delta t}{w} + \frac{t_2 - t_3}{w^2}\delta l + \frac{2\delta t}{(d_2 - d_1)} + 2\delta l\frac{(t_2 - t_1)}{(d_2 - d_1)^2}\right]. \tag{B2}$$

Typically, $d_2 - d_1 = 76$ mm (3 in.), $w = 10$ mm (0.4 in.), $t_2 - t_1 = 51$ μsec and $t_2 - t_3 = 3$ μsec, therefore $|\delta\langle c_1 \rangle/\langle c_1 \rangle| \cong 0.01$ or 1%.

2. *Attenuation measurements*
We recall eqn (4) for attenuation,

$$\langle\alpha\rangle = \ln(q)/(w_2 - w_1); \quad q = A_1/A_2. \tag{B3}$$

Let δA be the random error in measuring A_1 or A_2. Typically, $\delta A = 1/10$ divisions, A_1 and $A_2 = 2$ divisions, $w_2 - w_1 = 5$ mm and $\delta l = 0.0254$ mm; therefore,

$$\delta\langle\alpha\rangle/\langle\alpha\rangle = 2\delta A/(A \ln q) + 2\delta w/(w_2 - w_1). \tag{B4}$$

For the "worst" case, $q = 2.1$ and $\delta\langle\alpha\rangle/\langle\alpha\rangle = 0.15$; for the "best" case, $q = 7.2$ and $\delta\langle\alpha\rangle/\langle\alpha\rangle = 0.06$.